EPH - International Journal of Applied Science
ISSN (Online): 2208-2182
Volume 06 Issue 02-June, 2020

DOI: https://doi.org/10.53555/eijas.v6i2.97

INVESTIGATION OF THE INHIBITION OF COPPER AND A-BRASS CORROSION IN NITRIC ACID SOLUTIONS BY PISTACIA ATLANTICA EXTRACT

A. S. Foud[1] and A. A. Idress[2]*
[1]*Department of Chemistry, Faculty of Science, Mansoura University, Mansoura, Egypt.*
[*2]*Department of Chemistry, Faculty of Science, Omar Almukhtar University, Albayda, Libya.*

[*]***Corresponding Author:-***
Email: *asmaalasllai71@gmail.com*

Abstract:-
The detailed study of Pistacia Atlantica Extract (PAE) as corrosion inhibitor for copper and α-brass in nitric acid solution has been performed through potentio dynamic polarization, electrochemical impedance spectroscopy (EIS), electrochemical frequency modulation (EFM), scanning electron microscopy (SEM) and energy dispersive X-ray (EDX) measurements. The effect of inhibitor concentration and immersion time against inhibitor action was investigated. Results show that PAE may be used as an efficient inhibitor for copper and α-brass in nitric acid solutions. Potentiodynamic polarization studies reveal that PAE acts as a mixed type inhibitor without any change in the mechanism of hydrogen evolution.

Keywords: - *Copper, α-Brass, Corrosion inhibition, Pistacia Atlantica, Potentiodynamic polarization, EIS, EFM, SEM, EDX.*

INTRODUCTION

Copper and its alloys, because of their excellent resistance to corrosion in neutral aggressive media and their ease of processing, they are widely used in industries[1],especially in electronics, solar cell fittings, household products, structural engineering, art and decoration, coinage and biomedical application. Roughly, 19% of the weight of a mobile phone nowadays consists of copper and copper alloys. Even though copper is corrosion resistant due to its natural oxide film, it is prone to corrode in solutions that contain oxygen and high concentration of chloride, sulphate, sulphide and nitrate ions. A variety of potentially damaging environments require versatile inhibition actions. Although an inhibitor is sometimes added to avoid tarnishing, in the majority of cases the inhibitor's EPH - International Journal of Applied Science | ISSN: 2208-218229 purpose is to prevent or postpone corrosion attack. Numerous investigations have been conducted on the corrosion inhibition of copper and its alloys [2–11].

The surface of brass is chemically, physically and energetically heterogeneous [12] for several reasons which facilitate the corrosive process to operate on the surface. The extent of this reaction depends on the nature of the corrosive environment and the type of cathodic process [13]. HNO_3 is an oxidizing acid and its oxidizing capacity depends on its concentration. Metals react with nitric acid by giving hydrogen and the metal nitrates. The evolved hydrogen is used up in reducing nitric acid to various products [14]. It is known [15] that most of the brasses metals react with nitric acid to form hydrogen rich compounds (NH_3 or NH_2OH), whereas noble metals like silver or copper produce compounds rich in oxygen (NO_2, NO and HNO_2).

It is noticed that presence of hetero-atom such as nitrogen, sulphur, phosphorous in the organic compound molecule improves its action as copper corrosion inhibitor. Amongst these organic compounds and their derivatives such as azoles [16, 17], amino acids [18] and many others, but these compounds are highly toxic. Recently, the research is oriented to the development of green corrosion inhibitors, compounds with good inhibition efficiency but low risk of environmental pollution [19]. Plant extracts have attracted attention in the field of corrosion inhibition for many decades. As natural products, they are a source of non-toxic, eco-friendly, readily available and renewable inhibitors for preventing metal corrosion [20, 21].

Pistacia is widely distributed in Mediterranean Europe, Libya, and Morocco and in the west through southern France, Turkey, Iraq and Iran. The resin part of this plant known as Mastic resin and plant called as mastic tree [22]. It has a great medicinal value and already been used in traditional system of medicines like Unani and Ayurveda system [23].The most important component of *Pistacia* are resin which was analysed by GC & GC-MS to obtain α- pinene, β- pinene, limonene, terpene-4-ol and terpeneol[24].

The aim of the present work is to systematically study the inhibition of corrosion on copper and brass by Pistacia Atlantica extract in nitric acid solution. Chemical and different electrochemical techniques were explored and complemented by surface analytical techniques, scanning electron microscope (SEM) and energy dispersive X-ray (EDX).

EXPERIMENTAL

Materials and solutions

Experiments were performed using Copper specimens (99.98%) and α-brass (60-40 copper-zinc) were mounted in Teflon. An epoxy resin was used to fill the space between 30 Teflon and copper and also α-brass electrode. The aggressive solution used was prepared by dilution of analytical reagent grade 70% HNO_3 with bidistilled water. The stock solution (2000 ppm) of PAE was used to prepare the desired concentrations by dilution with bidistilled water. The concentration range of PAE used was 50-300 ppm.

Preparation of plant extracts

Fresh aerial parts of Pistacia Atlantica were collected from green mountain, Libya, in spring (June 2013). The Plant materials were shade dried at room temperature for 13 days. The shade dried plant materials of Pistacia Atlantica were crushed to make fine powder. The powdered materials (100 g each) were soaked in 250 ml of methanol for 5 days and then subjected to repeated extraction with 25× 30 ml until exhaustion of plant materials. The extracts obtained were then concentrated under reduced pressure using rotary evaporator at temperature below 55°C. The methanol evaporated to give solid extract that was prepared for application as corrosion inhibitor.

Electrochemical measurements

Electrochemical measurements were performed in three-electrode glass cell at constant temperature of 25 ± 1 ºC, a platinum electrode was used as counter electrode, and saturated calomel electrode (SCE) was used as reference electrode. The working electrode was embedded in epoxy resin, leaving a geometrical surface area of 1 cm^2 exposed to the electrolyte. Potentiodynamic (Tafel) polarization curves and electrochemical impedance measurements were carried out using a computer controlled Gamry Instrument PCI4-G750 Potentiostat/Galvanostat/ZRA. This includes a Gamry Framework system based on the ESA400, Gamry applications that include dc105 for dc corrosion measurements, EIS300 for electrochemical impedance spectroscopy and EFM 140 for electrochemical frequency modulation measurements along with a computer for collecting data. Echem Analyst 5.58 software was used for plotting, graphing and fitting data.

Accordingly all experiments were carried out after 30 minute immersion of metal specimens into the electrolyte. Tafel polarization curves were obtained using a sweep rate of 1 mV s^{-1} in the potential range from -1000 mV to 1200mV with respect to the open circuit potential. The linear Tafel segments of the anodic and cathodic curves were extrapolated to

corrosion potential to obtain the corrosion current densities. Then i_{corr} was used for the calculation of inhibition efficiency and surface coverage (θ) as below [25]:

$$\%\,IE = \theta \times 100 = \left(1 - \frac{i_{corr(inh)}}{i_{corr(free)}}\right) \times 100 \qquad (1)$$

Where $i_{corr(free)}$ and $i_{corr(inh)}$ are the corrosion current densities in the absence and presence of inhibitor, respectively.
Electrochemical impedance spectra were obtained in the frequency range of 100 kHz to 0.1 Hz with perturbation amplitude of 5 mV at the corrosion potential. The efficiency of the inhibition and the surface coverage (θ) obtained from the impedance measurements are defined by the following relations:

$$\%\,IE = \theta \times 100 = \left(1 - \left[\frac{R^{\circ}_{ct}}{R_{ct}}\right]\right) \times 100 \qquad (2)$$

Where R^{o}_{ct} and R_{ct} are the charge transfer resistance in the absence and presence of inhibitor, respectively.
Electrochemical frequency modulation, EFM, was carried out using two frequencies of 2 and 5 Hz. The base frequency was 0.1 Hz, so that the wave form repeats after 1 s. The intermodulation spectra contain current responses assigned for harmonical and intermodulation current peaks. The larger peaks were used to calculate the corrosion current density (i_{corr}), the Tafel slopes (β_c and β_a) and the causality factors CF-2 & CF-3.

Surface examination

Examination of copper and brass surface after 24 h exposure to the 1 M HNO_3 solution without and with PAE was carried out by Hitachi S-550 Scanning Electron Microscope. Rough elemental analyses for the exposed surface were conducted by EDX technique.

RESULTS AND DISCUSSION

Polarization Curves

Figure (1) shows the potentiodynamic polarization curves for copper dissolution in 1 M HNO_3 in the absence and presence of different concentrations of PAE at 25°C. Similar curves were obtained for other brass (Figure (2)). The numerical values of the variation of the corrosion current density (i_{corr}), the corrosion potential (E_{corr}), Tafel slopes (β_a and β_c), the degree of surface coverage (θ), and the inhibition efficiency (%IE) with different concentrations of inhibitor for copper and brass are given in Table (1). The potentiodynamic curves show that there is a clear reduction of both anodic and cathodic currents in the presence of inhibitor compared to those for the blank solution. It is clear that the cathodic 32 reduction (hydrogen evolution) and the anodic reaction (metal dissolution) were inhibited. The values of cathodic Tafel slope (β_c) for inhibitor are found to increase in the presence of inhibitor. The Tafel slope variation suggests that the investigated inhibitor influence the kinetic of the hydrogen evolution reaction [26]. This indicates an increase in the energy barrier for proton discharge, leading to less gas evolution [27]. The approximately constant values of β_a for inhibitors indicate that these compounds were first adsorbed onto the electrode (copper and brass) surface and impeded by merely blocking the reaction sites of the electrode surface without affecting the anodic reaction mechanism [28]. The small changes in corrosion potential, E_{corr}, which indicate that this extract is act as mixed type but mainly cathodic inhibitors for copper and brass corrosion in 1 M HNO_3 solution.

Table 1. Effect of concentration of PAE on the electrochemical parameters calculated by potentiodynamic polarization technique for the corrosion of copper and brass in 1 M HNO_3 at 25±1°C.

	Conc., ppm	i_{corr}, µA cm 2	$-E_{corr}$, mV vs. SCE	β_a, $Vdec^{-1}$	β_c, $Vdec^{-1}$	CR, mpy	θ	%IE
Copper	1 M HNO_3	379.0	-17.60	102.2	221	173.	---	---
	50	181.0	2.220	91.2	234	82.8	0.522	52.2
	100	163.0	-2.840	90.9	234	76.5	0.570	57.0
	150	126	4.090	107.8	220	57.6	0.668	66.8
	200	75.7	-25.80	85.4	282	34.5	0.800	80.0
	250	51.7	26.20	106.4	160.7	23.6	0.864	86.4
	300	33.80	14.60	87.2	188	15.4	0.91	91
α-Brass	1 M HNO3	1860.0	50.30	95.2	346.30	921.2	---	---
	50	222.0	46.50	103.0	246.80	109.9	0.881	88.1
	100	129.0	42.90	91.9	193.30	64.19	0.931	93.1
	150	109	49.50	97.3	209.90	54.19	0.941	94.1
	200	87.5	24.40	82.7	222.30	43.41	0.953	95.3
	250	75.7	40.50	86.4	232.00	37.53	0.959	95.9
	300	41.20	53.20	89.9	201.00	20.45	0.98	98

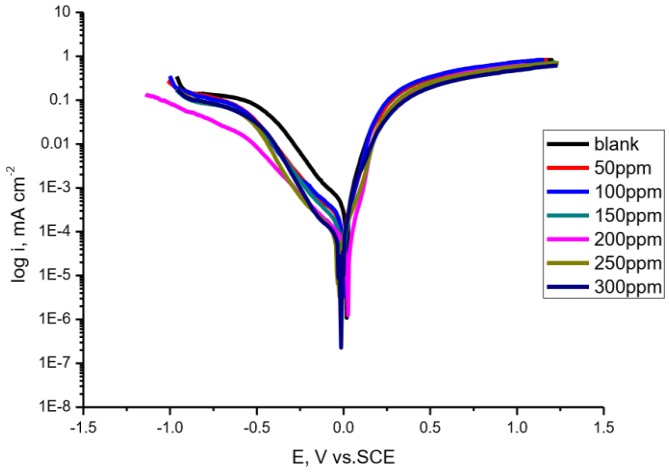

Figure 1. Potentiodynamic polarization curves for the corrosion of copper in 1 M HNO_3 solution with out and with various concentrations of PAE at 25±1˚C.

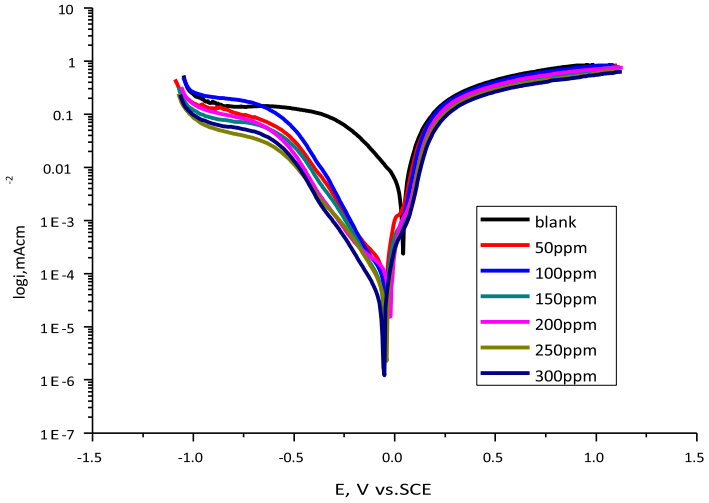

Figure 2. Potentiodynamic polarization curves for the corrosion of brass in 1 M HNO_3 solution without and with various concentrations of PAE at 25±1˚C.

Electrochemical impedance spectroscopy (EIS)

The corrosion behavior of copper and brass, in nitric acid solution, in the absence and presence of different concentrations of PAE, is also investigated by EIS at 25 °C after 30 min of immersion Figures (3-6). EIS spectra of the these compounds were analyzed using the equivalent circuit in Figure 7, where R_s represents the solution resistance, R_{ct} denotes the charge-transfer resistance, and a CPE instead of a pure capacitor represents the interfacial capacitance [29]. The impedance of a CPE is described by the following equation:

$$Z_{CPE} = Y_0^{-1}(j\omega_{max})^{-n} \qquad (3)$$

Where Y0 is the magnitude of the CPE, j is an imaginary number, ω is the angular frequency ($\omega_{max} = 2\pi f_{max}$), f_{max} is the frequency at which the imaginary component of the impedance reaches its maximum values, and n is the deviation parameter of the CPE: $-1 \leq n \leq 1$. The values of the interfacial capacitance C_{dl} can be calculated from CPE parameter values Y_0 and n using equation [30]:

$$C_{dl} = Y_0(\omega_{max})^{n-1} \qquad (4)$$

After analyzing the shape of the Nyquist plots, it is concluded that the curves approximated by a single capacitive semicircles, showing that the corrosion process was mainly charged-transfer controlled [31, 32]. The general shape of the curves is very similar for all samples (in presence or in absence of inhibitors at different immersion times) indicating that no change in the corrosion mechanism [33].

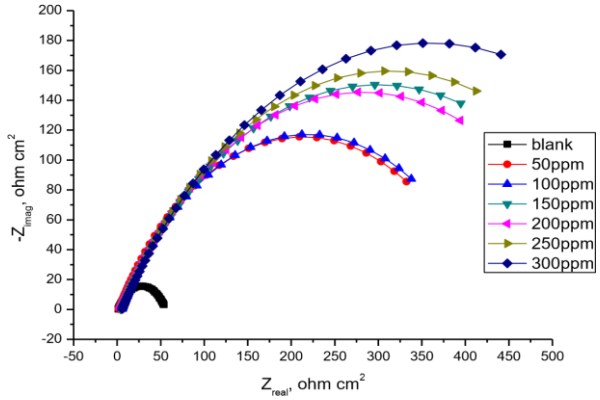

Figure 3. Nyquist plots recorded for copper in 1 M HNO_3 without and with various concentrations of PAE at 25±1˚C.

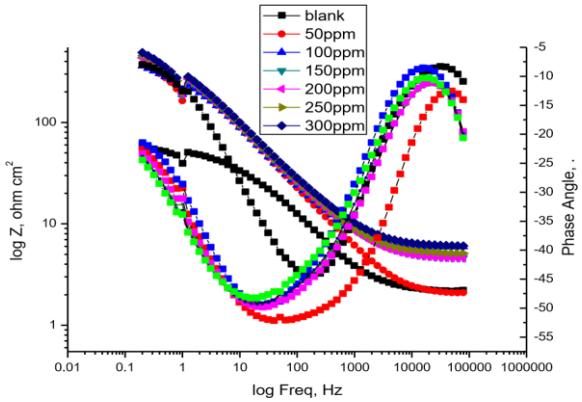

Figure 4. Bode plots recorded for copper in 1 M HNO_3 without and with various concentrations of PAE at 25±1˚C.

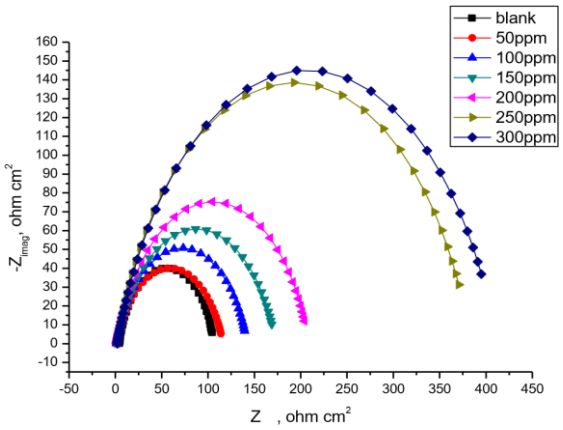

Figure 5. Nyquist plots recorded for brass in 1 M HNO_3 without and with various concentrations of PAE at 25±1°C.

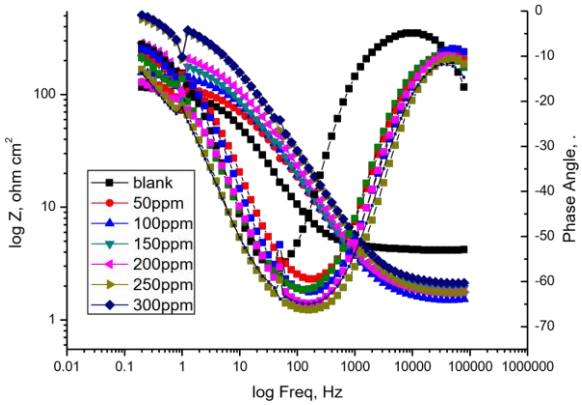

Figure 6. Bode plots recorded for brass in 1 M HNO_3 without and with various concentrations of PAE at 25±1˚C.

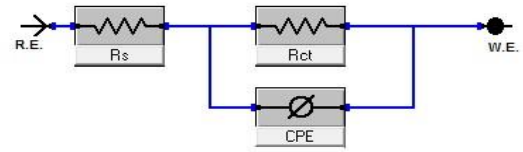

Figure 7. Electrical equivalent circuit used to fit the impedance data

The charge-transfer resistance (R_t) values are calculated from the difference in impedance at lower and higher frequencies. The double layer capacitance (C_{dl}) and the frequency at which the imaginary component of the impedance is maximal (-Zmax) are determined. The impedance parameters derived from these investigations are summarized in Table 2. The results obtained from Table 2 reveals that the presence of the PAE led to decreasing the values of C_{dl} due to the decrease of the local dielectric constant and/or from the increase of thickness of the electrical double layer. It was suggested that the inhibitor molecules were functioned by adsorption at the metal / solution interface. Thus, the decrease in C_{dl} values and the increase in R_{ct} values and consequently, the inhibition efficiency may be reported as the gradual replacement of water molecules by the adsorption of the inhibitor molecules from the metal surface, and by decreasing the extent of dissolution reaction.

Table 2. Electrochemical kinetic parameters obtained from EIS technique for copper and brass in 1 M HNO_3 solution containing various concentrations of PAE at 25±1˚C.

	Conc., ppm,	R_{ct}, Ω cm^2	C_{dl}, µF cm^{-2}	θ	%IE
Copper	1 M HNO_3	53.51	270	--	--
	50	426.70	401	0.875	87.5
	100	423.90	393	0.874	87.4
	150	556.60	477	0.904	90.4
	200	591.00	555	0.909	90.9
	250	615.00	540	0.913	91.3
	300	701.00	596	0.924	92.4
α-Brass	1 M HNO3	102.10	281	--	--
	50	114.40	1	0.404	40.4
	100	140.70	0	0.274	27.4
	150	171.30	0	0.507	50.7
	200	207.00	0	0.108	10.8
	250	381.90	0	0.733	73.3
	300	410.20	0	0.751	75.1

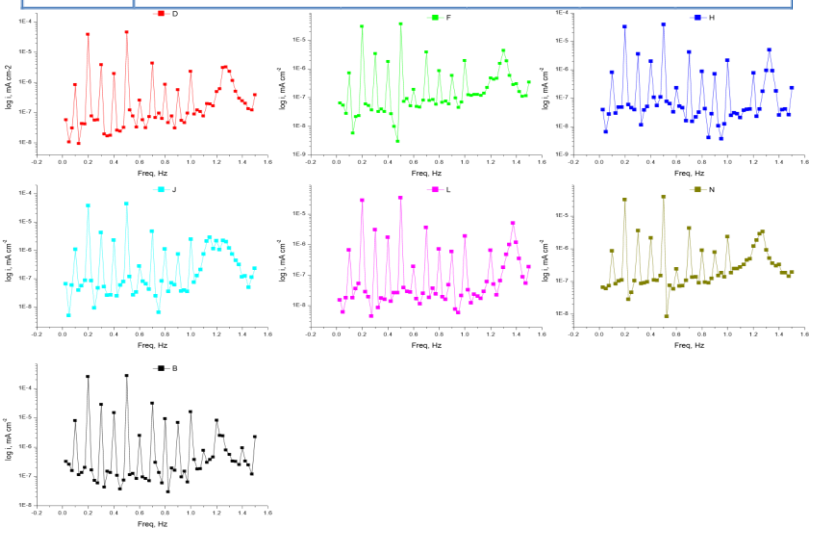

Figure 8. EFM spectra for copper in the absence and presence of different concentrations of PAE in 1 M HNO_3. (D 50ppm, F 100ppm, H 150ppm, j 200ppm, L 250ppm, N 300ppm, B blank).

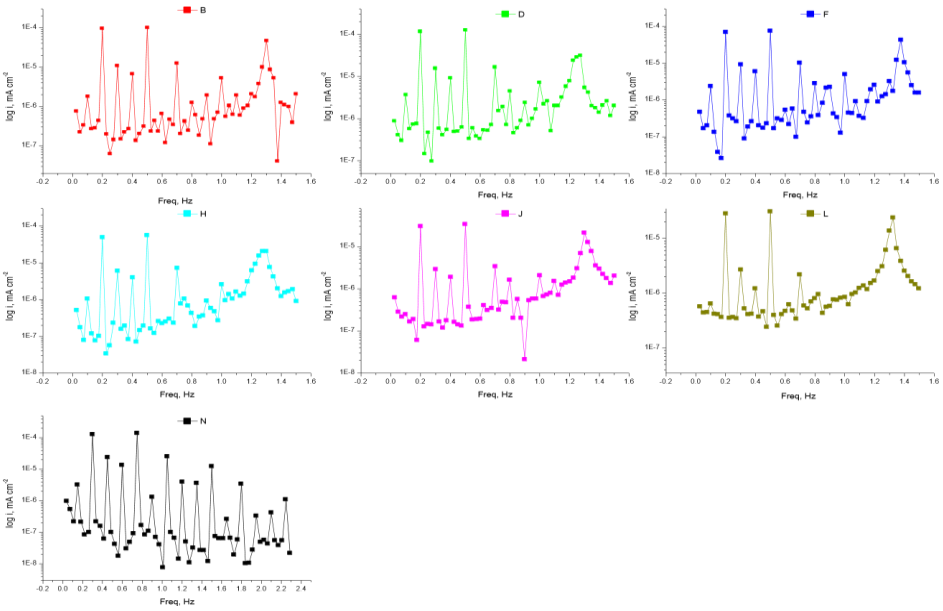

Figure 9. EFM spectra for brass in the absence and presence of different concentrations of PAE in 1 M HNO_3. (B 50ppm, D100ppm, F 150ppm, H 200ppm, J 250ppm, L300ppm, N blank).

Electrochemical frequency modulation technique (EFM)

The result of EFM experiments is a spectrum of current response as a function of frequency. The spectrum is called the 'intermodulation spectrum'. Figures (17, 18) show the corresponding current response in the intermodulation spectrum for copper and brass in 1M HNO_3 at 25± 1 °C respectively. Electrochemical kinetic parameters calculated from EFM for copper and brass in 1M HNO_3 are listed in Table (3). Table (3) shows the corrosion kinetic parameters such as inhibition efficiency (IE_{EFM} %), corrosion current density (µA cm^{-2}), Tafel constants (βa, βc) and causality factors (CF-2, CF-3) at different concentration of PAE in 1M HNO_3 at 25 ±1. It is obvious from Table (3) that, the corrosion current densities decrease by increasing the concentrations of PAE. The inhibition efficiencies increase by increasing PAE concentrations. The causality factors in Table (3) are very close to the 40 theoretical values which according to the EFM theory [34, 35] should guarantee the validity of Tafel slopes and corrosion current densities. Inhibition efficiency (IE_{EFM} %) depicted in Table (3).

It is clear from Table (3) that the corrosion current densities decrease with increase in PAE concentrations. Values of the causality factors in Table (3) indicate that the measured data are of good quality. The standard values for CF-2 and CF-3 are 2.0 and 3.0, respectively. The causality factors are calculated from the frequency spectrum of the current response. If the causality factors differ significantly from the theoretical values of 2.0 and 3.0, then it can be deduced that the measurements are influenced by noise. If the causality factors are approximately equal to the predicted values of 2.0 and 3.0, i.e. there is a causal relationship between the perturbation signal and the response signal. Then the data are assumed to be reliable [36]. The great strength of the EFM is the causality factors which serve as an internal check on the validity of the EFM.

Table 3. Electrochemical kinetic parameters obtained by EFM technique for copper and brass in 1 M HNO_3 solution containing different concentrations of PAE at 25±1˚C.

	Conc., ppm	i_{corr}, µA cm^{-2}	βa, $mVdec^{-1}$	βc, $mVdec^{-1}$	CR, mm y^{-1}	CF-2	CF-3	θ	%IE
Copper	1 M HNO_3	291.1	57	95	143.70	1.96	3.44	----	----
	50	66.52	78	150	32.83	1.92	2.88	0.771	77.1
	100	48.32	71	133	23.89	1.93	2.46	0.834	83.4
	150	47.29	67	120	23.34	1.85	3.40	0.837	83.7
	200	44.28	57	90	21.85	1.88	2.94	0.847	84.7
	250	43.25	69	162	21.34	1.84	3.43	0.851	85.1
	300	42.68	62	110	21.06	1.76	4.30	0.853	85.3
α-Brass	1 M HNO_3	199.30	63	215	98.33	1.88	2.94	----	----
	50	152.3	16.3	74	75.15	1.95	1.28	0.236	23.6
	100	119.1	88.5	51	58.78	1.75	2.84	0.608	60.8
	150	78.21	96.4	54.7	38.78	2.00	3.78	0.745	74.5
	200	50.83	81.4	50	25.08	2.00	3.78		74.5
	250	37.48	99.4	62	18.49	1.59	769.60	0.812	81.2
	300	30.6	81.6	58	15.10	2.30	1.10	0.846	84.6

SEM/EDX examination

The SEM image of the surface of copper and brass free before immersion in 1 M HNO_3 surface showing the clear polishing lines is almost free from corrosion (Figures 10a, 11a), while after immersion in 1 M HNO_3 the surface is corded and damaged by acid (Figures 10b, 11b) and finally after immersion in 1 M HNO_3 and the presence of 300 ppm of PAE the surface is protected and we observed a much lower density of pits at the materials surface compared with sample in 1 M HNO_3 (Figures 10c, 11c). EDX spectrum of copper and brass free show high peak of copper and zinc as shown in Figures (11a, 12a), while in the presence of 1M HNO_3, the rate of corrosion is increased, and the reduced intensity of copper peak of EDX spectrum (Figures 11b, 12b) is due to the increase of corrosion products(copper oxides). For the solution containing PAE(300ppm), the EDX spectrum showed increase again in copper and zinc peak compared with sample in 1 M HNO_3 (Figures 11c, 12c) and presence of carbon peak which indicate that the inhibitor molecules have adsorbed on the metal surface, so the protection of metal surface is confirmed.

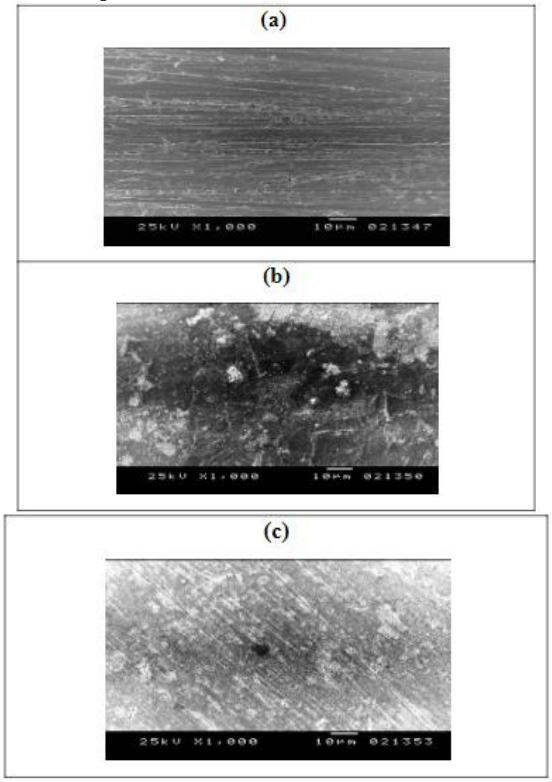

Figure 10. SEM micrographs of copper surface (a) before of immersion in 1 M HNO_3, (b) after 24 h of immersion in 1 M HNO_3 and (c) after 24 h of immersion in 1 M HNO_3+ 300 ppm PAE at 25±1 °C.

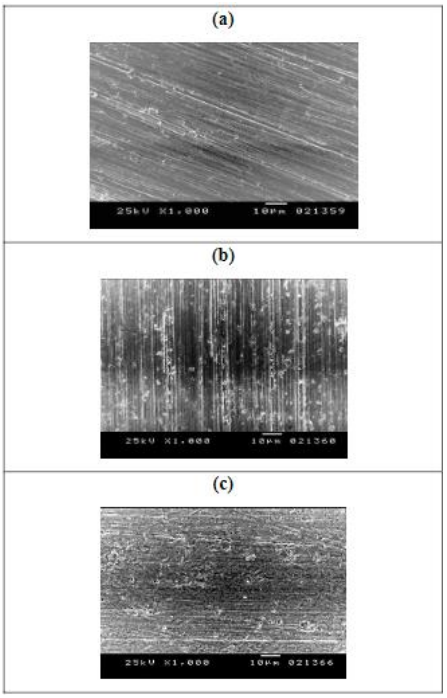

Figure 11. SEM micrographs of brass surface (a) before of immersion in 1 M HNO_3, (b) after 24 h of immersion in 1 M HNO_3 and (c) after 24 h of immersion in 1 M $HNO_3$4.

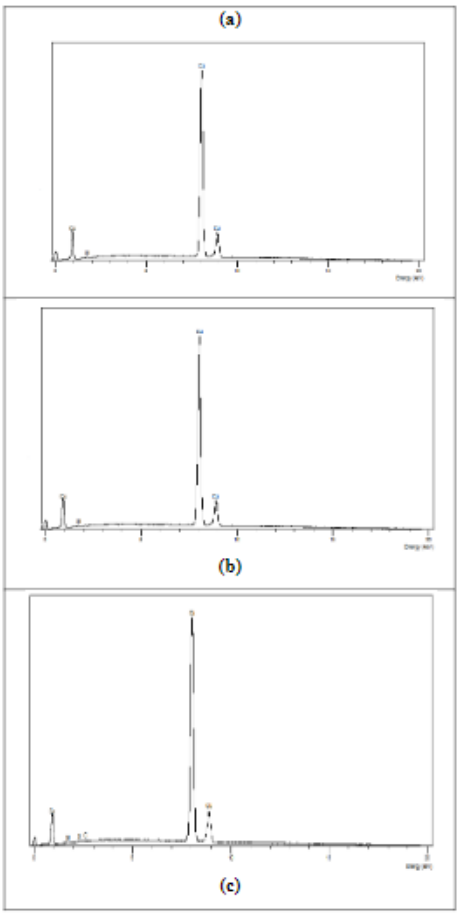

Figure12. EDX spectra of copper surface (a) before of immersion in 1 M HNO_3, (b) after 24 h of immersion in 1 M HNO_3 and (c) after 24 h of immersion in 1 M HNO_3+ 300 ppm PAE at 25±1 °C.

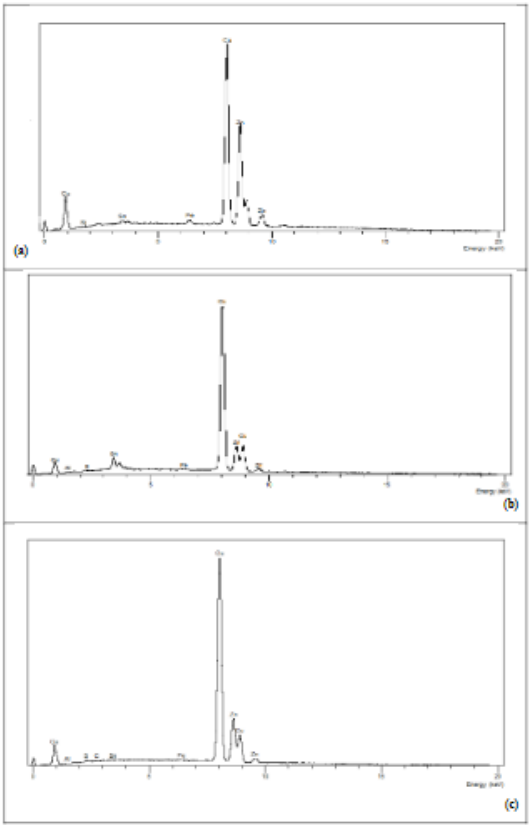

Figure 13. EDX spectra of brass surface (a) before of immersion in 1 M HNO_3, (b) after 24 h of immersion in 1 M HNO_3 and (c) after 24 h of immersion in 1 M HNO_3+ 300 ppm CSE at 25±1 °C

Table4. Surface composition (wt %) of copper and bass before and after immersion in 1 M HNO_3 without and with 300 ppm of PAE at 25±1 °C.

	(Mass %)	Cu	Zn	Si	S	Fe	Al	Sn	C
Copper	Copper alone	99.6	--	0.4	--	--	--	--	--
	Copper + 1 M HNO_3	98.9	--	0.5	0.3	--	0.3	--	--
	Copper + 1 M HNO_3 + 300 ppm PAE	99.0	--	0.3	0.1	--	0.4	--	0.2
α-Brass	α-Brass alone	63.4	34.4	0.3	--	1.1	--	0.8	--
	α-Brass + 1 M HNO_3	62.8	34.1	--	0.5	0.9	0.4	1.3	--
	α-Brass + 1 M HNO_3 + 300 ppm PAE	63.4	34.3	--	0.2	1.0	0.3	0.5	0.3

CONCLUSIONS

From the overall experimental results the following conclusions can be deduced:

1. PAE shows good inhibitive action against the corrosion of copper and brass in 1 M HNO_3.
2. The value of inhibition efficiency increases with increasing the inhibitor concentration.
3. PAE is good inhibitor and act mixed type but mainly cathodic inhibitors for copper and brass corrosion in 1 M HNO_3 solution.
4. There is good agreement between the data obtained from electrochemical methods.

REFERENCES

[1].**Schweitzer, P., (2010)**. Fundamentals of Corrosion: Mechanisms, Causes, and Preventative Methods, CRC Press,Taylor and Francis Group, LLC, New York, USA,**.**

[2].**Ameh, P.O, Oyeniyi, Q.S** and **Sani, U.M., (2015)**. Quantum Chemical Studies on the Corrosion Inhibitions of Mild Steel in Acidic Medium by 5-amino-1- cyclopropyl-7-[(3R,5S)-3,5-dimethylpiperazin-1-yl]-6,8-difluoro-4-oxo-1,4dihydroquinoline-carboxylic acid. International Journal of Chemical, Material and Environmental Research, 2 (3): 1

[3].**Bentiss, M.**, **Traisnel, M.**, and **Lagrenee, M., (2001)**. Influence of 2, 5-bis (4Dimethylaminophenyl)- 1, 3, 4-Thiadiazole on Corrosion Inhibition of Mild Steel in Acidic Media. Journal of Applied Electrochemistry, 31, 41 – 50.

[4].**Ishwara J., Vijaya DPA, (2011)**. A study of aluminum corrosion inhibition in Acid medium by antiemetic drug. Springer 64(4-5):377-384.

[5].**Obot I.B.,** and **Obi-Egbedi N.O., (2010)**. Adsorption properties and inhibition of mild steel corrosion in sulphuric acid solution by ketoconazole: Experimental and theoretical investigation. Corros. Sci., 52, 198–204.

[6].**Song P., Guo X.-Y.**, **Pan Y.-C.**, **Shen S.**, **Sun Y.**, **Wen Y.**, and **Yang H.-F.**, **(2013)**. Insight in cysteamine adsorption behaviors on the copper surface by electrochemistry and Raman spectroscopy. Electrochim, 89, 503–509.

[7].**Ameh, P.O., Oyeniyi, Q.S** and **Sani, U.M.,(2015)**. Quantum Chemical Studies on the Corrosion Inhibitions of Mild Steel in Acidic Medium by 5-amino-1- cyclopropyl-7-[(3R,5S)-3,5-dimethylpiperazin-1-yl]-6,8-difluoro-4-oxo-1,4dihydroquinoline-3- carboxylic acid. Int. J. Chem. Mater. Environ. Res., 2 (3): 1-16.

[8].**Sastri V.S., (1998)**. Corrosion Inhibitors Principles and Applications. Wiley, Chichester.

[9].**García, S.J., Muster, T.H.**, **Özkanat, Ö. Sherman,. N.**, **Hughes,A.E.** ,**Terryn,H. J.H.W. de Wit, J.M.C**. **Mol,(2010)**. The influence of pH on corrosion inhibitor selection for 2024-T3 aluminium alloy assessed by high-throughput multielectrode and potentiodynamic testing. ElectrochimicaActa, vol. 55, pp. 2457-2465.

[10]. **Roberge,P. R.** Handbook of corrosion engineering. New York: McGraw Hill Handbook.

[11]. **Arslan, T., Kandemirli, F., Ebenso, E.E.**, **Love, I.** and **Alemu, H.**, **(1999).** Quantum chemical studies on the corrosion inhibition of some sulphonamides on mild steel in acidic medium. Corrosion Science, 2009, 51: 35–47.

[12]. **Pang, X.**, **Ran, X.**, **Kuang, F.**, **Xie, J.** and **Hou, B. (2010).** Inhibiting effect of ciprofloxacin, norfloxacin and ofloxacin on corrosion of mild steel in hydrochloric acid. Chinese Journal of Chemical Engineering, 18: 337–345.

[13]. **Singh, A.K.**, **Shukla, S.K.**, **Singh, M.** and **Quraishi, M.A., (2011)**. Inhibitive effect of ceftadizime on corrosion of mild steel in hydrochloric acid solution. Material, Chemistry and Physics, 129: 68–76.

[14]. **Ameh, P.O** and **Sani, U.M.** Cefuroxime Axetil: **(2015)**. A Commercially Available Pro-Drug as Corrosion Inhibitor for Aluminum in Hydrochloric Acid Solution. Journal of Heterocyclics, 101: 1-6.

[15]. **Gece, G.,(2011).** Drugs: A review of promising novel corrosion inhibitors. Corrosion Science, 53: 3873–3898.

[16]. **Mahdi, A.S. (2014)**. Amoxicillin as green corrosion inhibitor for concrete reinforced steel in simulated concrete pore solution containing chloride, (IJARET), 5, 99- 107.

[17]. **Pathak,R. K. P.**, **Mishra,(2016)**. Drugs as Corrosion Inhibitors: A Review. International Journal of Science and Research, Volume 5 Issue 4, 671- 677.

[18]. **Scendo, M.,(2007)**. Inhibitive action of the purine and adenine for copper corrosion in sulphate solutions. Corrosion Science, 49, 2985–3000.

[19]. **Evans, U.R., (1960)**. The Corrosion and Oxidation of Metals. Arnold, London, p. 324.

[20]. **Fenelon, M., Breslin, C.B., (2001)**. An Electrochemical study of the formation of Benzotriazole surface films on Copper, Zinc and a Copper–Zinc alloy. J. Appl. Electrochem. 31, 509–516.

[21]. **Fouda, A.S., Shalabi, K.**, **Elewady, G.Y.**, **Merayyed H.F., (2014)**. Chalcone derivatives as corrosion inhibitors for carbon steel in 1 M HCl solutions. Int. J. Electrochem. Sci., 9, 7038.
[22]. **Fouda, A.S., Shalabi, K., Idress , A.A., (2014)**. Thymus Vulgarise Extract as Nontoxic Corrosion Inhibitor for Copper and α-Brass in 1 M HNO3. Int. J. Electrochem. Sci., 9, 5126–5154.
[23]. **Kertit, S., Essoufi, H., Hammouti, B., Benkaddour, (1998)**. 1 -phenyl-5-mercaptol, 2, 3,4-tétrazole (PMT) : un nouvel inhibiteur de corrosion de l'alliage Cu-Zn efficace à très faible concentration. **M.** Chim. Phys**.** 95**, 2070–2082.**
[24]. **Kliskic M., Radosevic, J., Gndic,S., (1997)**. Pyridine and its derivatives as inhibitors of aluminium corrosion in chloride solution. J. Appl. Electrochem. 27, 947.
[25]. **Li, X.H., Deng, S.D., Fu, H., Mu G.N., (2010)**. Synergistic inhibition effect of rare earth cerium (IV) ion and sodium oleate on the corrosion of cold rolled steel in phosphoric acid solution, Corros. Sci. 52, 1167.
[26]. **Quartarone G., Moretti G., Bellomi T., Capobianco G., Zingales A., (1998).** Using Indole to Inhibit Copper Corrosion in Aerated 0.5 M Sulfuric Acid. Corrosion. 54, 606.
[27]. **Bjorndahl W.D., Nobe K., (1984)**. Copper Corrosion in Chloride Media. Effect of OxygenCorrosion. 40, 82.
[28]. **R. Schumacher., A. Muller W., Stockel., (1987).** An in situ study on the mechanism of the electrochemical dissolution of copper in oxygenated sulphuric acid: An application on the quartz n microbalance. J,Electroanal. Chem. 219, 311.
[29]. **Silverman D.C.**, **(1988)** Corrosion. Electrochemical Impedance Technique — a Practical Tool for Corrosion Prediction. J.E. Carrico, 44,280.
[30]. **W.J. Lorenz, F. Mansfeld., (1981).** Determination of corrosion rates by electrochemical DC and AC methods, Corros. Sci. 21 647.
[31]. **D.D. Macdonald, M.C. Mckubre.,(1982)**. Impedance measurements in electrochemical systems, Modern Aspects of Electrochemistry. Vol. 14, Plenum Press, New York, , p. 61
[32]. **Mansfeld F., (1981).** Recording and Analysis of AC Impedance Data for Corrosion Studies, Corrosion, 36**. 130.**
[33]. **Gabrielli C.**, **(1980)**. Identification of Electrochemical processes by Frequency Response Analysis. Solarton Instrumentation Group.
[34]. **El Achouri M., Kertit S., Gouttaya H.M., Nciri B., Bensouda Y., Perez L., Infante M.R., Elkacemi K., (2001).** Corrosion inhibition of iron in 1 M HCl by some gemini surfactants in the series of alkanediyl-α, ω-bis-(dimethyl tetradecyl ammonium bromide). Prog. Org. Coat, 43, 267.
[35]. **Macdonald J.R.,. Johanson W.B, (1987).** Theory in Impedance Spectroscopy, John Wiley& Sons, New York.
[36]. **Mertens S.F., Xhoffer C., Decooman B.C., Temmerman E.**, **(1997).** Corrosion Short-Term Deterioration of Polymer-Coated 55% Al-Zn — Part 1: Behavior of Thin Polymer Films. 53, 381.